Bulletin of Pure and Applied Sciences
Zoology (Animal Science), Vol.41A, No.1,
July-December 2022: P.320-336

Print version ISSN 0e70 0765
Online version ISSN 2320 3188

Computational Evaluation of Potent Alkaloids as Promising CDK2 Inhibitors

A.A. Kazi*
Department of Pharmaceutical Chemistry, N.B.S. Institute of Pharmacy, Ausa, Latur, Maharashtra, India
Corresponding Author E-mail: kaziaasim@gmail.com

Abstract
Cyclin-dependent kinase 2 (CDK2) plays a crucial regulatory role in cell-cycle progression, making it an attractive target for anticancer drug development. In this study, six bioactive alkaloids—berberine, evodiamine, matrine, piperine, sanguinarine, and tetrandrine—were computationally evaluated to identify potent CDK2 inhibitors. The selected molecules, chosen for their well-documented anticancer activities, were subjected to a systematic workflow comprising molecular docking, ADMET prediction, drug-likeness assessment, and environmental toxicity analysis. Molecular docking performed using PyRx and AutoDock Vina revealed that several alkaloids exhibit strong binding affinity toward CDK2, with sanguinarine (–10.3 kcal/mol), evodiamine (–9.8 kcal/mol), and berberine (–9.3 kcal/mol) outperforming the native ligand. Their superior interactions were attributed to favorable hydrogen bonding, electrostatic forces, and extensive hydrophobic contacts within the CDK2 active site. ADMET analysis conducted through SwissADME and ADMETlab 3.0 demonstrated that evodiamine, piperine, and matrine possess balanced pharmacokinetic properties, while berberine and sanguinarine showed moderate oral absorption and acceptable safety profiles. Drug-likeness evaluation indicated full compliance with Lipinski's rules for all compounds, with evodiamine and matrine exhibiting the highest QED values. Toxicity modeling highlighted moderate risks for certain molecules; however, the potent compounds remained within manageable safety margins. Environmental toxicity assessment further differentiated the compounds based on bioaccumulation and aquatic toxicity potential. Overall, the integrated computational approach identified sanguinarine, evodiamine, and berberine as the most promising CDK2 inhibitors. Their strong binding affinities, supportive ADMET characteristics, and favorable drug-likeness profiles warrant further experimental validation to advance them as potential anticancer therapeutic candidates.

Keywords: CDK2 inhibitors, alkaloids, molecular docking, ADMET analysis, drug-likeness, anticancer agents, computational modeling.

Graphical Abstract

Bulletin of Pure and Applied Sciences
Zoology (Animal Science), Vol.41A, No.1,
July-December 2022: P.320-336

Print version ISSN 0e70 0765
Online version ISSN 2320 3188

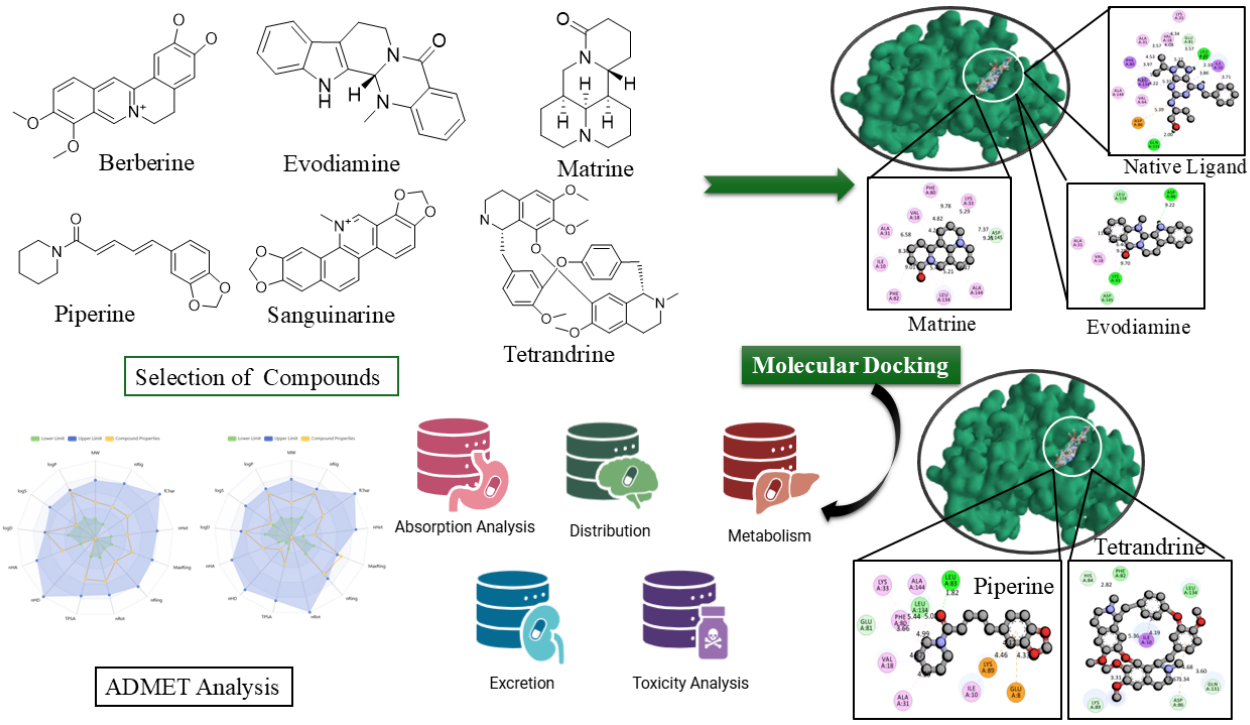

Introduction

Cancer remains one of the leading causes of morbidity and mortality worldwide, driven largely by uncontrolled cell proliferation and dysregulation of key molecular pathways that govern the cell cycle. Among the numerous proteins implicated in cell-cycle control, cyclin-dependent kinase 2 (CDK2) has emerged as a central regulatory enzyme responsible for coordinating the G1/S transition and DNA synthesis (1–3). CDK2 forms active complexes with cyclins E and A, enabling the phosphorylation of substrates essential for DNA replication and cell-cycle progression. Aberrant activation or overexpression of CDK2 has been observed in various malignancies, including breast, lung, colon, ovarian, and prostate cancers, where it contributes to unchecked proliferation, genomic instability, and therapeutic resistance. Consequently, CDK2 has gained prominence as an attractive molecular target for anticancer drug development, prompting extensive interest in designing selective inhibitors that can modulate its activity (4,5). Natural products, particularly plant-derived secondary metabolites, continue to play a significant role in modern drug discovery due to their structural diversity, biological relevance, and favorable pharmacological properties (6,7). Among these, alkaloids constitute one of the most widely studied classes of bioactive phytochemicals(8–10). Alkaloids such as berberine, evodiamine, matrine, piperine, sanguinarine, and tetrandrine have been extensively documented for their anticancer potential, exhibiting activities that include apoptosis induction, cell-cycle arrest, inhibition of metastasis, disruption of signaling pathways, and suppression of angiogenesis (11,12). Their multifaceted mechanisms of action and structural adaptability make them compelling candidates for further evaluation as CDK2 inhibitors. Advances in computational chemistry have revolutionized early-stage drug discovery by enabling rapid, cost-effective screening of molecular interactions between potential therapeutic candidates and biological targets. Techniques such as molecular docking, pharmacokinetic prediction, and toxicity modeling provide detailed insights into the binding behavior, drug-likeness, and overall suitability of compounds before they progress to experimental validation. Molecular docking, in particular, allows the

Print version ISSN 0e70 0765
Online version ISSN 2320 3188

prediction of ligand–protein interactions by estimating binding conformations and affinity within the active site of the target protein. When combined with in silico ADMET (Absorption, Distribution, Metabolism, Excretion, and Toxicity) analysis, these approaches help identify compounds with optimal pharmacokinetic properties and minimal safety liabilities (13,14). The assessment of drug-likeness further refines the selection process by evaluating physicochemical features aligned with successful oral drugs, such as those defined by Lipinski's rule of five. Additionally, environmental toxicity modeling is increasingly recognized as a crucial component of early drug development, ensuring that the designed molecules do not pose ecological hazards that could limit their therapeutic advancement. Computational strategies therefore provide a comprehensive framework for identifying candidates with both therapeutic potential and acceptable safety profiles. Given the pharmacological significance of alkaloids and the therapeutic relevance of CDK2 inhibition, a systematic computational evaluation of selected natural alkaloids is warranted. Such an approach not only supports the identification of promising lead molecules but also enhances understanding of their molecular interactions, predicted bioavailability, and potential toxicity (15,16). This study aims to explore the inhibitory potential of six bioactive alkaloids against CDK2 using an integrated in silico methodology, providing valuable insights that may guide future experimental and medicinal chemistry efforts toward developing novel anticancer agents.

Method Section

Selection of compound

In this study, six bioactive alkaloids—berberine, evodiamine, matrine, piperine, sanguinarine, and tetrandrine—were selected for computational evaluation as potential CDK2 inhibitors. These compounds were chosen based on extensive literature evidence highlighting their strong anticancer properties, favorable pharmacological profiles, and documented effects on key molecular pathways associated with cell-cycle regulation.

Berberine is widely reported to inhibit tumor proliferation through modulation of MAPK, PI3K/AKT, JAK/STAT, and NF-κB signaling pathways. Evodiamine exhibits potent antiproliferative activity by inducing apoptosis, suppressing metastasis, and inhibiting topoisomerase-related pathways. Matrine has demonstrated anticancer efficacy by promoting apoptosis and regulating Bcl-2 family proteins, along with inducing cell-cycle arrest. Piperine is known to enhance cytotoxicity, inhibit cancer cell migration, and improve the bioavailability of other anticancer agents. Sanguinarine is a strong inducer of ROS-mediated apoptosis, mitochondrial dysfunction, and caspase activation, contributing to pronounced antiproliferative effects. Tetrandrine, a bis-benzylisoquinoline alkaloid, has shown significant inhibitory effects on cancer progression by suppressing calcium-dependent signaling, inducing autophagy, and blocking cell-cycle progression (17). Collectively, these alkaloids represent diverse structural classes with established anticancer potential, making them suitable candidates for computational screening against CDK2 in the present study

Molecular Docking

Molecular docking was conducted to evaluate the binding affinity and interaction profiles of the selected phytoconstituents against the target protein. The chemical structures of all ligands were initially sketched and energy-minimized using ChemDraw, followed by conversion into compatible 3D formats. Canonical SMILES and additional structural attributes (100.864692, 101.746577, and 79.892615) were retrieved from PubChem to ensure structural accuracy and uniformity prior to docking. The optimized ligand structures were imported into PyRx 0.9, where they were subjected to energy minimization using the Universal Force Field (UFF).

Print version ISSN 0e70 0765
Online version ISSN 2320 3188

AutoDock Vina, integrated within PyRx, was employed as the docking engine. The target protein structure was prepared by removing crystallographic water molecules, adding polar hydrogens, and repairing incomplete residues (18–20). Grid box dimensions were defined to fully encompass the active site, ensuring unbiased exploration of all potential binding pockets. Docking simulations were performed with default Vina parameters, and the best poses were selected based on binding affinity scores (kcal/mol). The resulting protein–ligand complexes were further analyzed using Biovia Discovery Studio Visualizer, which enabled detailed visualization of hydrogen bonding, hydrophobic interactions, π–π stacking, and other non-covalent contacts within the binding pocket. This integrative workflow ensured reliable prediction of ligand–receptor interactions and facilitated the identification of compounds with the most promising molecular docking profiles.

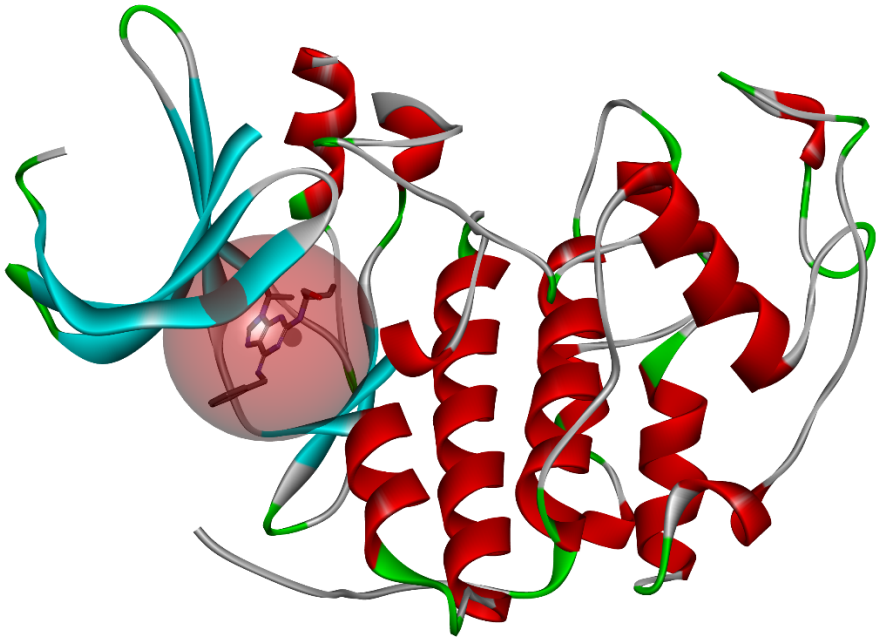

Figure 1. 3D line ribbon representation of cyclin-dependent kinase 2 with Native Ligand

ADMET Analysis

Absorption, Distribution, Metabolism, Excretion, and Toxicity (ADMET) profiling of the selected phytoconstituents was performed using a combination of computational tools to predict drug-likeness and pharmacokinetic suitability. Initially, the two-dimensional structures of all compounds were drawn and energy-optimized using ChemDraw, ensuring accurate stereochemistry and molecular geometry. The canonical SMILES and physicochemical descriptors for each compound were subsequently retrieved from PubChem to standardize molecular input parameters. The obtained molecular structures were screened through SwissADME, which provided detailed predictions of physicochemical properties, lipophilicity (logP), water solubility (logS), gastrointestinal absorption, bioavailability score, and compliance with drug-likeness filters such as Lipinski, Ghose, Veber, Egan, and Muegge criteria. Parameters such as topological

Print version ISSN 0e70 0765
Online version ISSN 2320 3188

polar surface area (TPSA), number of rotatable bonds, hydrogen bond donors, and acceptors were also assessed to estimate membrane permeability and oral absorption potential. Further toxicity and pharmacokinetic evaluation was conducted using ADMETlab 3.0, which generated quantitative predictions for parameters including plasma protein binding, blood–brain barrier penetration, cytochrome P450 interactions, hepatotoxicity, mutagenicity, and acute toxicity indices. Environmental toxicity descriptors, bioaccumulation factors, and in-silico LD50 values were also examined to ensure comprehensive safety assessment (21,22). Together, these computational approaches provided an integrated ADMET profile for each compound, enabling systematic comparison of their drug-likeness, pharmacokinetic behavior, and toxicity risks to support their selection for downstream molecular docking and therapeutic evaluation.

Results and Discussion

Molecular Docking

The molecular docking analysis of selected alkaloids against cyclin-dependent kinase 2 (CDK2) revealed significant variations in binding affinities and interaction profiles, highlighting their potential as CDK2 inhibitors **figure 2**. The native ligand exhibited a docking score of –8.3 kcal/mol, forming key stabilizing interactions with residues such as ASP86, LEU83, GLN131, PHE80, and ILE10, thus serving as a reference for evaluating the inhibitory potential of the tested compounds. Among the alkaloids, sanguinarine demonstrated the highest binding affinity with a docking score of –10.3 kcal/mol, surpassing the native ligand. Its strong interaction pattern included attractive electrostatic interactions with ASP145 and a conventional hydrogen bond with THR14. Hydrophobic (Pi–Sigma) interactions with ILE10 and multiple contacts with LEU134 further stabilized the complex, suggesting a strong propensity to occupy the CDK2 active pocket. Evodiamine also showed excellent affinity (–9.8 kcal/mol), supported by carbon hydrogen bonding with ASP145 and robust hydrophobic interactions involving LEU134, ALA144, and VAL64. The presence of Pi-Sigma and Pi-Alkyl contacts indicates a well-fitted orientation within the hydrophobic region of the active site. Berberine displayed a docking score of –9.3 kcal/mol, forming stabilizing hydrogen bonds with GLY13 and hydrophobic interactions with LEU134, VAL18, and ILE10. These interactions suggest a stable ligand orientation and favorable binding energy, ranking berberine as another strong CDK2 inhibitor candidate. Matrine and piperine showed moderate but still significant interactions, each with docking scores of –8.6 kcal/mol. Matrine primarily stabilized through alkyl interactions with VAL64, LEU134, ILE10, and VAL18, whereas piperine formed a strong conventional hydrogen bond with LEU83 and notable electrostatic interactions (Pi-cation with LYS89 and Pi-anion with GLU8). These interactions reflect their moderate affinities and possible role as supplementary CDK2 modulators. Among all compounds, tetrandrine showed the weakest binding (–7.5 kcal/mol), despite forming several hydrogen bonds with ASP86, HIS84, GLN131, and LYS89. Hydrophobic interactions with ILE10 and Pi-anion interactions with ASP86 contributed to stability, but the overall affinity remained lower than other alkaloids. Overall, the docking results indicate that sanguinarine, evodiamine, and berberine exhibit superior binding affinities compared with the native ligand, driven mainly by strong electrostatic attractions, hydrogen bonding, and extensive hydrophobic interactions. These findings suggest that these alkaloids can effectively target the CDK2 active site and may serve as promising leads for developing novel CDK2 inhibitors for anticancer applications.

Table 1. Binding interactions of selected compounds with cyclin-dependent kinase 2

Print version ISSN 0e70 0765
Online version ISSN 2320 3188

Amino Acid	**Bond Length**	**Bond Type**	**Bond Category**	**Ligand Energy (Kcal/mol)**	**Docking Score**
Native Ligand					
ASP86	5.38961	Electrostatic	Attractive Charge	547.18	-8.3
LEU83:O	2.40512	Hydrogen Bond	Conventional Hydrogen Bond		
LEU83	2.09865				
GLN131	1.99657				
GLU81	3.57321		Carbon Hydrogen Bond		
PHE80	3.97441	Hydrophobic	Pi-Sigma		
ILE10	3.86369				
ILE10	3.70681				
LEU134	3.97159				
LEU134	3.90371				
VAL64	4.22471		Alkyl		
LEU134	5.47012				
ALA144	4.17475				
VAL18	4.07836				
ALA31	3.57268				
LYS33	4.3413				
VAL18	5.21804		Pi-Alkyl		
PHE80	4.52821				
Berberine					
GLY13	3.33661	Hydrogen Bond	Carbon Hydrogen Bond	403.87	-9.3
LEU134	3.91575	Hydrophobic	Pi-Sigma		
VAL18	4.17582		Alkyl		
ILE10	5.26492		Pi-Alkyl		
VAL18	4.57209				
ALA31	4.94595				
Evodiamine					
ASP145	3.59246	Hydrogen Bond	Carbon Hydrogen Bond	1258.05	-9.8
LEU134	3.78286	Hydrophobic	Pi-Sigma		
LEU134	5.29332		Alkyl		
LEU134	4.94902		Pi-Alkyl		
ALA144	4.28381				
ALA31	4.97335				
VAL64	5.13603				

Print version ISSN 0e70 0765
Online version ISSN 2320 3188

ALA144	4.21683				
Matrine					
VAL64	4.87404	Hydrophobic	Alkyl	341.16	-8.6
LEU134	5.42622				
ILE10	5.36835				
VAL18	4.82339				
LYS33	5.29351				
VAL18	4.26169				
LEU134	5.20788				
ALA144	3.84715				
PHE80	4.35149		Pi-Alkyl		
Piperine					
LEU83	1.81775	Hydrogen Bond	Conventional Hydrogen Bond	302.35	-8.6
GLU81	3.65974		Carbon Hydrogen Bond		
LYS89	4.11538	Electrostatic	Pi-Cation		
GLU8	4.33496		Pi-Anion		
VAL18	4.86835	Hydrophobic	Alkyl		
ALA31	4.25204				
LYS33	5.43828				
ALA144	5.07722				
ILE10	4.46039		Pi-Alkyl		
PHE80	4.99468				
Sanguinarine					
ASP145	5.13198	Electrostatic	Attractive Charge	561.95	-10.3
THR14	2.6483	Hydrogen Bond	Conventional Hydrogen Bond		
GLU81	3.4525		Carbon Hydrogen Bond		
ASP145	3.78503				
ILE10	3.97382	Hydrophobic	Pi-Sigma		
LEU134	3.79645				
LEU134	3.66384				
Tetrandrine					
ASP86	3.66605	Hydrogen Bond	Carbon Hydrogen Bond	754.58	-7.5
HIS84	2.81738				
ASP86	3.33569				
GLN131	3.59836				
LYS89	3.31447				
ASP86	4.68242	Electrostatic	Pi-Anion		

Print version ISSN 0e70 0765
Online version ISSN 2320 3188

ILE10	3.46323	Hydrophobic	Pi-Sigma		
ILE10	4.18733		Alkyl		
ILE10	5.35596		Pi-Alkyl		

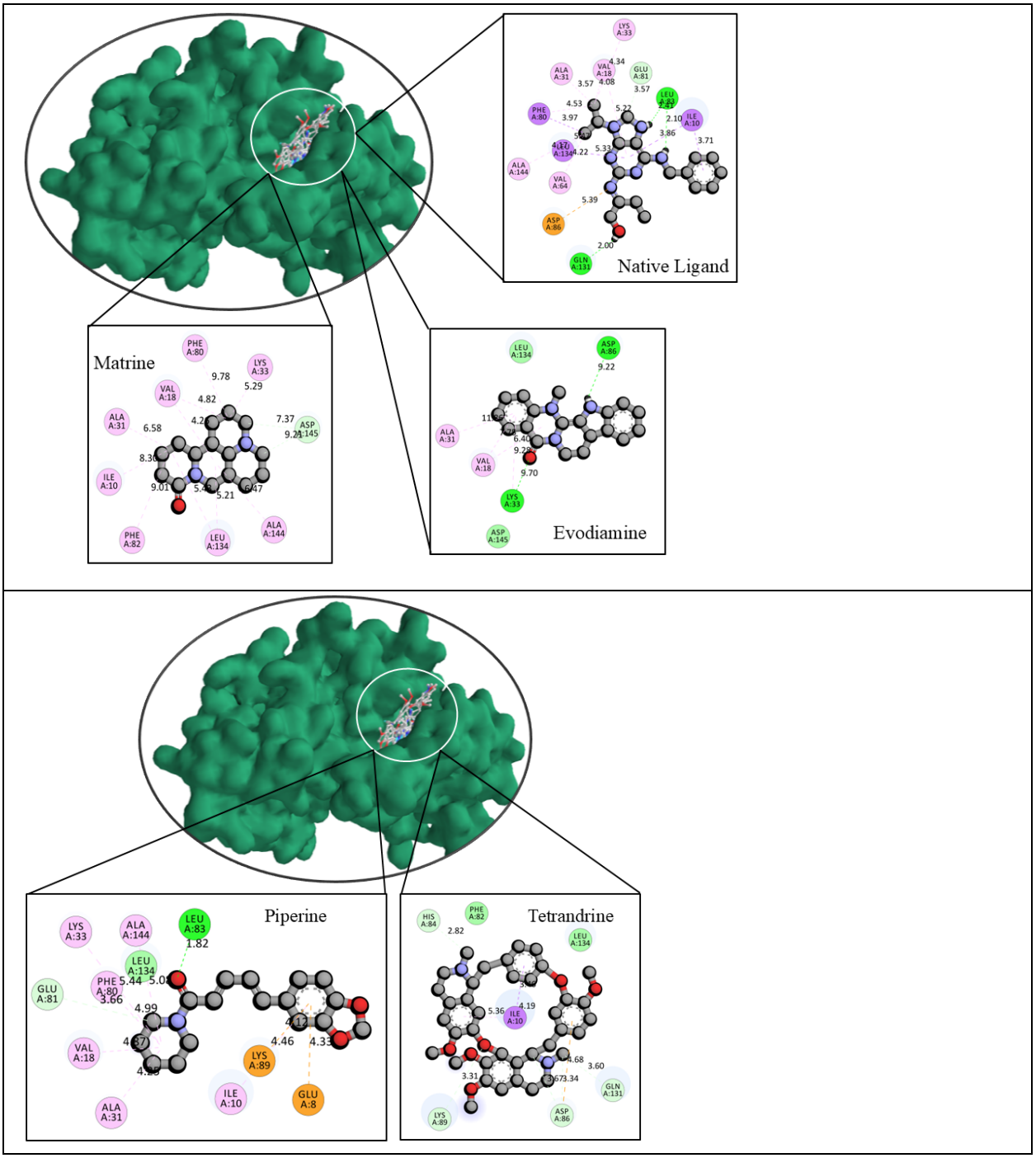

Figure 2. The 2D and 3D binding interaction poses of the most potent Compounds with cyclin-dependent kinase 2 enzyme

ADMET Analysis

Bulletin of Pure and Applied Sciences
Zoology (Animal Science), Vol.41A, No.1,
July-December 2022: P.320-336

Print version ISSN 0e70 0765
Online version ISSN 2320 3188

The ADMET assessment shows that most compounds have suitable molecular weights, such as berberine (318.1), evodiamine (303.14), and piperine (285.14), supporting good absorption, while tetrandrine (622.3) may show reduced permeability. TPSA values indicate varying permeability: matrine (23.55 Å²) and piperine (38.77 Å²) favor membrane diffusion, whereas the native ligand (87.89 Å²) and berberine (80.05 Å²) are less permeable. LogP values of piperine (2.50), evodiamine (2.53), and berberine (2.80) fall in the optimal range, while matrine (1.33) is more hydrophilic. Solubility is lowest for sanguinarine (logS –5.74) and highest for matrine (–1.84). Overall, piperine and evodiamine present the most balanced ADMET profiles.

Table 2. Physicochemical properties of selected derivatives

Compounds	**MW**	**Volume**	**Dense**	**nHA**	**nHD**	**nRot**	**nRing**	**TPSA**	**logS**	**logP**
Native ligand	354.22	367.8264	0.963009	7	3	8	3	87.89	-4.84894	3.995874
berberine	318.1	316.5973	1.004746	5	0	7	2	80.05	-4.14758	2.801201
evodiamine	303.14	315.0867	0.962084	4	1	0	5	39.34	-3.58261	2.535292
matrine.	248.19	261.9177	0.947588	3	0	0	4	23.55	-1.8409	1.337658
piperine.	285.14	298.4675	0.955347	4	0	4	3	38.77	-3.90497	2.509494
sanguinarine.	332.09	326.8852	1.015922	5	0	0	6	40.8	-5.74045	3.606714
tetrandrine	622.3	649.0061	0.958851	8	0	4	8	61.86	-4.71681	3.605032

Drug-likeness assessment showed that all compounds fully complied with the Lipinski, Golden Triangle, and Chelator rules, indicating suitable physicochemical characteristics and no major liabilities for oral drug development. The QED values demonstrated that evodiamine (0.692), matrine (0.653), and piperine (0.633) possess the most favorable drug-like profiles, even higher than the native ligand (0.576), suggesting strong potential for further optimization. In contrast, sanguinarine (0.365) and especially tetrandrine (0.238) exhibited low QED scores, reflecting less desirable drug-likeness.Natural product complexity was evident from the NP Scores, where tetrandrine (1.667), matrine (1.171), and sanguinarine (1.059) showed high NP values, indicating structural richness commonly associated with strong bioactivity. However, this also correlated with alerts in Pfizer and GSK rules for sanguinarine and tetrandrine, suggesting possible issues related to lipophilicity or toxicity.

Bulletin of Pure and Applied Sciences
Zoology (Animal Science), Vol.41A, No.1,
July-December 2022: P.320-336

Print version ISSN 0e70 0765
Online version ISSN 2320 3188

Table 3. Drug-likeness properties of designed derivatives

Compounds	QED	NP Score	Lipinski rule	Pfizer Rule	GSK Rule	Golden Triangle	Chelator Rule
Native ligand	0.576	-0.747	0	0	0	0	0
berberine	0.455	-1.447	0	0	0	0	0
evodiamine	0.692	0.166	0	0	0	0	0
matrine	0.653	1.171	0	0	0	0	0
piperine	0.633	0.125	0	0	0	0	0
sanguinarine	0.365	1.059	0	1	0	0	0
tetrandrine	0.238	1.667	0	1	1	1	0

The absorption profiles of the selected compounds demonstrated considerable variation in permeability, efflux susceptibility, and predicted human intestinal absorption (HIA). Caco-2 and MDCK permeability values indicated that all compounds exhibit moderate to low passive permeability, with tetrandrine and evodiamine showing relatively better permeation (around –4.61 to –4.59), while the native ligand exhibited the lowest permeability (–5.29 to –5.08). P-gp interaction analysis revealed that most compounds act as strong P-gp inhibitors, including the native ligand, berberine, piperine, and tetrandrine, which may enhance intracellular accumulation. However, sanguinarine and native ligand showed strong P-gp substrate tendencies, suggesting susceptibility to efflux and reduced absorption. Conversely, matrine demonstrated minimal P-gp inhibition and moderate substrate probability, indicating low efflux involvement. The HIA values showed very low predicted absorption for most molecules, except evodiamine (0.010), piperine (0.0036), and sanguinarine (0.0137), which exhibited comparatively higher intestinal uptake potential. The fraction absorbed (F20%, F30%, F50%) highlighted better absorption for the native ligand and tetrandrine across multiple thresholds, whereas berberine and matrine showed poor absorption efficiency.

Table 4. Absorption parameter of selected compounds

Compounds	Caco-2 Permeability	MDCK Permeability	Pgp-inhibitor	Pgp-substrate	HIA	F20%	F30%	F50%
Native ligand	-5.29131	-5.08421	0.996207	0.000101	0.000132	0.022361	0.992657	0.978368
berberine	-4.70981	-4.6189	0.970076	3.06E-06	0.002816	0.000766	0.039478	0.767635
evodiamine	-4.63479	-4.59794	0.962228	0.720104	0.010483	0.055741	0.596943	0.939191
matrine.	-4.78797	-4.95094	0.023491	0.312502	1.99E-05	0.002055	0.081941	0.054161

Print version ISSN 0e70 0765
Online version ISSN 2320 3188

piperine.	-4.73117	-4.6696	0.990762	0.003481	0.003663	0.109595	0.011374	0.364159
sanguinarine.	-4.97531	-4.71088	1.23E-05	0.999581	0.013747	0.720534	0.327034	0.99841
tetrandrine	-4.61182	-4.66721	0.92162	0.579462	0.000447	0.347228	0.350452	0.994397

The distribution analysis revealed substantial variability among the selected compounds. Plasma protein binding (PPB%) was high for most molecules, particularly piperine (98%), evodiamine (96%), and berberine (92%), indicating limited free drug availability in circulation. In contrast, matrine showed the lowest PPB (11%), resulting in the highest unbound fraction (Fu 87.9%), suggesting greater tissue accessibility. Volume of distribution (VD) values were generally low to moderate, with berberine and sanguinarine showing relatively higher distribution compared to the native ligand. BBB permeability was notable for evodiamine (0.73) and tetrandrine (0.94), indicating significant CNS penetration potential, whereas sanguinarine and piperine had very low BBB entry. Metabolic profiling based on CYP450 interactions indicated diverse metabolic pathways. Most compounds acted as strong CYP1A2 and CYP3A4 inhibitors, particularly the native ligand, berberine, and piperine, suggesting possible drug–drug interaction risks. Matrine demonstrated minimal CYP inhibition but remained a substrate for multiple isoforms, indicating extensive metabolic turnover. Evodiamine, sanguinarine, and tetrandrine showed broad substrate tendencies across CYP2C19, CYP2C9, CYP2D6, and CYP3A4, reflecting multi-pathway metabolism.

Table 5. Distribution and metabolism parameter of selected molecules

Compounds	**Distribution**				**Metabolism**									
					CYP1A2		**CYP2C19**		**CYP2C9**		**CYP2D6**		**CYP3A4**	
	PPB%	**VD**	**BBB**	**Fu**	**Inhibitor**	**Substrate**	**Inhibitor**	**Substrate**	**Inhibitor**	**Substrate**	**Inhibitor**	**Substrate**	**Inhibitor**	**Substrate**
Native ligand	75.05422	0.016597	0.124659	19.48986	0.999874	0.59594	0.059013	0.086452	0.999425	0.124496	0.99706	0.205607	0.999753	0.000301
berberine	91.99773	0.214781	0.040683	6.287566	0.999731	0.043158	0.999929	0.057038	0.999923	1.22E-05	3.63E-06	2.54E-05	0.936513	0.99376
evodiamine	96.10511	0.060681	0.730561	4.641536	0.204817	0.988071	0.999649	0.995965	0.987499	0.006643	0.000286	0.054784	0.962297	0.999978
matrine.	11.23014	-0.00204	0.238594	87.92352	6.20E-09	0.968039	1.23E-05	0.999996	1.16E-09	2.10E-11	0.521779	0.9737	0.01314	0.999999

Print version ISSN 0e70 0765
Online version ISSN 2320 3188

piperine.	98.00567	-0.19398	0.109937	1.893588	0.999995	0.811113	0.316511	0.2391	0.043279	0.050652	0.999762 2	0.999995	0.984327	0.0007
sanguinarine.	65.11207	0.103807	0.012045	37.87719	1	0.999995	0.999972	0.998513	0.028329	0.99999	0.999997	0.999977	1	0.115263
tetrandrine	75.01015	0.15237 6	0.940531	23.62958	0.000232	1	2.75 E-05	0.999999	4.70 E-05	0.999183	0.001264	0.999999	0.017445	0.999979

The excretion analysis of the selected compounds revealed notable differences in clearance and half-life. Tetrandrine displayed the highest plasma clearance (9.23) and the longest half-life (2.56 h), indicating prolonged systemic exposure. Matrine also showed an extended half-life (1.95 h), whereas berberine and piperine demonstrated shorter half-lives (<0.50 h), suggesting rapid elimination. The native ligand and evodiamine exhibited moderate clearance and half-life values, representing balanced excretion behavior. Toxicity predictions showed considerable variability. Hepatotoxicity (H-HT) and DILI risk were highest for evodiamine and the native ligand, while tetrandrine showed the lowest DILI probability, suggesting reduced liver toxicity. Ames toxicity remained low for most compounds except piperine and sanguinarine, which showed higher genotoxic potential. Rat oral acute toxicity indicated moderate toxicity for sanguinarine and evodiamine. FDAMDD values were elevated for tetrandrine and sanguinarine, indicating potential safety concerns. Skin sensitization was moderate for most compounds, while carcinogenicity was highest in sanguinarine and piperine, requiring caution for long-term use. Eye corrosion/irritation risk was extremely low for the native ligand but higher for berberine, sanguinarine, and tetrandrine. Respiratory toxicity predictions indicated higher risk for berberine and evodiamine.

Table 6. Excretion and Toxicity parameters of selected compounds

Compounds	**Excretion**		**Toxicity**									
	CL-plasma	**T1/2**	**H-HT**	**DILI**	**Ames Toxicity**	**Rat Oral Acute Toxicity**	**FDAMDD**	**Skin Sensitization**	**Carcinogenicity**	**Eye Corrosion**	**Eye Irritation**	**Respiratory Toxicity**
Native ligand	8.297629	0.810419	0.700608	0.953436	0.900551	0.068516	0.670867	0.89882	0.825187	3.65 E-09	0.041739	0.750169
berberine	5.045251	0.446098	0.156075	0.600238	0.162508	0.275118	0.240343	0.92384	0.194925	0.387296	0.839023	0.970151

Print version ISSN 0e70 0765
Online version ISSN 2320 3188

evodiamine	7.389529	0.989893	0.924523	0.976234	0.542349	0.737804	0.595334	0.955709	0.397179	0.000107	0.652814	0.935592
matrine.	7.014699	1.956742	0.579397	0.119967	0.499717	0.245532	0.372944	0.686417	0.515825	0.490816	0.878927	0.637463
piperine.	5.50535	0.470164	0.631062	0.79896	0.760771	0.272134	0.738733	0.606959	0.732121	0.00549	0.639499	0.748688
sanguinarine.	2.911932	0.55811	0.161298	0.818782	0.807573	0.826051	0.934141	0.92472	0.916587	0.001447	0.930735	0.912754
tetrandrine	9.237686	2.567326	0.580452	0.012365	0.648809	0.617789	0.955252	0.61972	0.814285	8.19 E-07	0.005789	0.74309

The environmental toxicity assessment of the designed molecules showed notable differences in ecological impact. Bioaccumulation potential (BCF) was highest for tetrandrine (2.25) and sanguinarine (1.98), indicating greater environmental persistence, while matrine (0.38) showed minimal accumulation risk. IGC50 values revealed that tetrandrine and sanguinarine exerted stronger toxicity toward green algae, whereas matrine exhibited the lowest inhibitory effects. Similar trends were observed in aquatic toxicity profiles. Fish toxicity (LC50FM) and Daphnia magna toxicity (LC50DM) were highest for sanguinarine and tetrandrine, highlighting their elevated toxicity to aquatic organisms. In contrast, matrine consistently showed the least toxicity in all environmental models.

Table 7. Environmental toxicity profile of designed molecules

Compounds	BCF	IGC50	LC50FM	LC50DM
Native ligand	1.349933	3.687039	4.455354	4.680451
berberine	1.029766	3.703506	4.817569	5.220547
evodiamine	1.527477	4.214102	5.019686	5.459352
matrine.	0.380249	2.761437	3.26381	4.053869
piperine.	1.004724	3.647	4.615218	5.2266
sanguinarine.	1.981364	4.413096	5.661905	6.21209
tetrandrine	2.250586	4.533112	5.347493	6.003566

Table 8. ADMET radar of most potent compounds and Native ligand

Bulletin of Pure and Applied Sciences
Zoology (Animal Science), Vol.41A, No.1,
July-December 2022: P.320-336

Print version ISSN 0e70 0765
Online version ISSN 2320 3188

Native Ligand

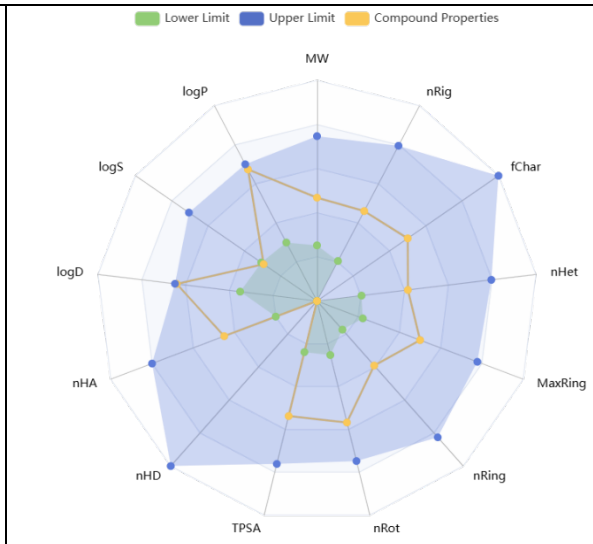

Berberine

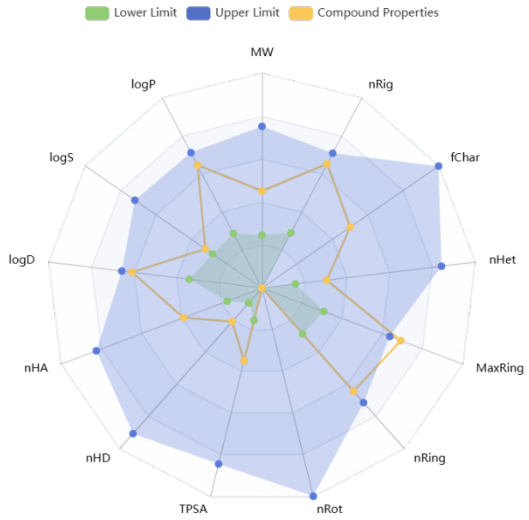

Evodiamine

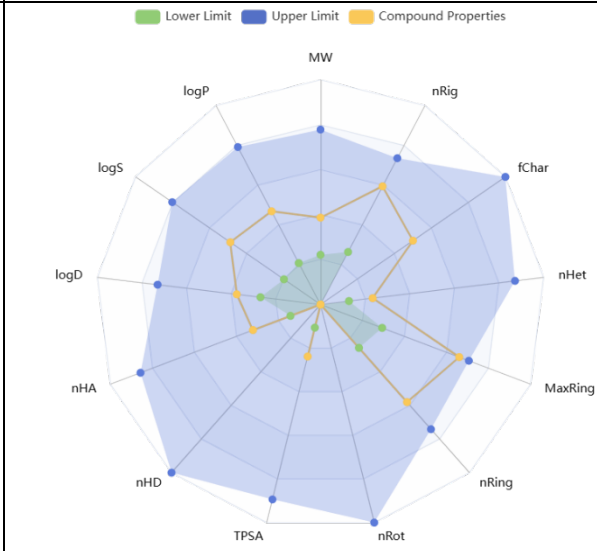

Matrine

Print version ISSN 0e70 0765
Online version ISSN 2320 3188

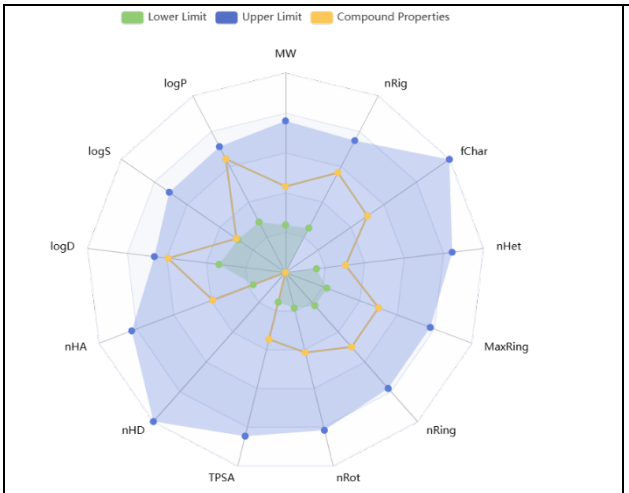

Piperine

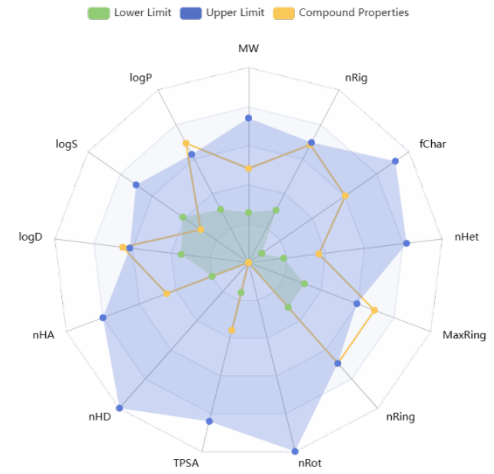

Sanguinarine

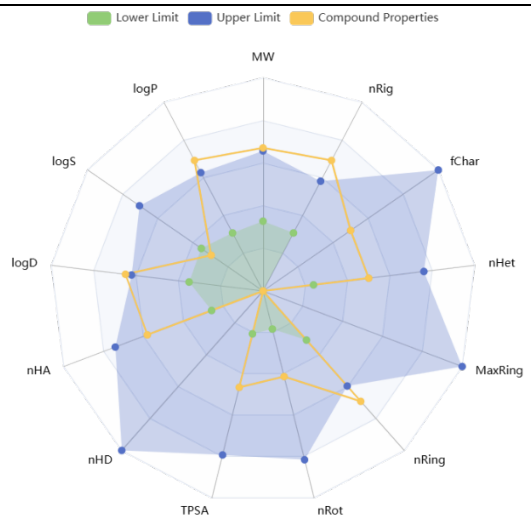

Tetrandrine

Conclusion

The comprehensive computational evaluation of six bioactive alkaloids against CDK2 demonstrates their strong potential as anticancer therapeutic candidates. Molecular docking revealed that sanguinarine, evodiamine, and berberine exhibit superior binding affinities compared with the native ligand, driven by robust hydrogen bonding, electrostatic forces, and extensive hydrophobic interactions within the CDK2 active site. Among them, sanguinarine showed the most remarkable affinity, followed closely by evodiamine and berberine, confirming their suitability as potent CDK2 inhibitors. ADMET and drug-likeness assessments further supported the pharmacokinetic feasibility of these compounds, with evodiamine and berberine showing balanced properties that favor potential oral bioavailability and metabolic stability. Although some toxicity and environmental concerns were noted for specific molecules, the overall profiles of the three potent

Print version ISSN 0e70 0765
Online version ISSN 2320 3188

alkaloids indicate manageable risks with appropriate optimization. Collectively, these findings highlight berberine, evodiamine, and sanguinarine as promising lead molecules for future anticancer drug development targeting CDK2. Their favorable binding behavior, structural diversity, and biologically relevant pharmacokinetic attributes warrant further in vitro and in vivo validation to advance them as viable therapeutic candidates.

References

1. Knudsen ES, Witkiewicz AK, Sanidas I, Rubin SM. Targeting CDK2 for cancer therapy. Vol. 44, Cell Reports. 2025.
2. Zeng Y, Ren X, Jin P, Fan Z, Liu M, Zhang Y, et al. Inhibitors and PROTACs of CDK2: challenges and opportunities. Vol. 19, Expert Opinion on Drug Discovery. 2024. p. 1125–48.
3. Arora M, Moser J, Hoffman TE, Watts LP, Min M, Musteanu M, et al. Rapid adaptation to CDK2 inhibition exposes intrinsic cell-cycle plasticity. Cell. 2023;186(12):2628-2643.e21.
4. Bai Y, Aodeng G, Ga L, Hai W, Ai J. Research Progress of Metal Anticancer Drugs. Vol. 15, Pharmaceutics. 2023.
5. Kumar G, Virmani T, Sharma A, Pathak K. Codelivery of Phytochemicals with Conventional Anticancer Drugs in Form of Nanocarriers. Vol. 15, Pharmaceutics. 2023.
6. Huang Y, Cao S, Zhang Q, Zhang H, Fan Y, Qiu F, et al. Biological and pharmacological effects of hexahydrocurcumin, a metabolite of curcumin. Vol. 646, Archives of Biochemistry and Biophysics. 2018. p. 31–7.
7. Zhang L, Yan M, Liu C. A comprehensive review of secondary metabolites from the genus Agrocybe: Biological activities and pharmacological implications. Vol. 15, Mycology. 2024. p. 162–79.
8. Onukwuli CO, zuchukwu CEI, Ugwu OPC. Exploring Phytochemicals for Diabetes Management: Mechanisms, Efficacy, and Future Directions. Newport Int J Res Med Sci. 2024;5(2):7–17.
9. Koche D, Shirsat R, Kawale M. An Overerview of Major Classes of Phytochemicals: Their Types and Role in Disease Prevention. Hislopia J. 2016;9(1/2):1–11.
10. Rozirwan, Nanda, Nugroho RY, Diansyah G, Muhtadi, Fauziyah, et al. Phytochemical composition, total phenolic content and antioxidant activity of Anadara granosa (Linnaeus, 1758) collected from the east coast of South Sumatra, Indonesia. Baghdad Sci J. 2023;20(4):1258–65.
11. He A, Wu M, Pu Y, Li R, Zhang Y, He J, et al. Fluoxetine as a Potential Therapeutic Agent for Inhibiting Melanoma Brain and Lung Metastasis: Induction of Apoptosis, G0/G1 Cell Cycle Arrest, and Disruption of Autophagy Flux. J Cancer. 2024;15(12):3825–40.
12. Smith JJ, Xiao Y, Parsan N, Medwig-Kinney TN, Martinez MAQ, Moore FEQ, et al. The SWI/SNF chromatin remodeling assemblies BAF and PBAF differentially regulate cell cycle exit and cellular invasion in vivo. PLoS Genet. 2021;18(1).
13. Swanson K, Walther P, Leitz J, Mukherjee S, Wu JC, Shivnaraine R V., et al. ADMET-AI: a machine learning ADMET platform for evaluation of large-scale chemical libraries. Bioinformatics. 2024;40(7).
14. Venkataraman M, Rao GC, Madavareddi JK, Maddi SR. Leveraging machine learning models in evaluating ADMET properties for drug discovery and development. ADMET DMPK. 2025;13(3).
15. Zuo Y, Zhang C zheng, Ren Q, Chen Y, Li X, Yang J rui, et al. Activation of mitochondrial-associated apoptosis signaling pathway and inhibition of PI3K/Akt/mTOR signaling pathway by voacamine suppress breast cancer progression. Phytomedicine. 2022;99.

Print version ISSN 0e70 0765
Online version ISSN 2320 3188

16. Saini N, Goswami V, Thakor E, Vasava M, Patel B. Anticancer Potential of Piperidine Containing Small Molecule Targeted Therapeutics. Vol. 9, ChemistrySelect. 2024.
17. Duda-Madej A, Viscardi S, Szewczyk W, Topola E. Natural Alkaloids in Cancer Therapy: Berberine, Sanguinarine and Chelerythrine against Colorectal and Gastric Cancer. Int J Mol Sci. 2024;25(15).
18. Shaheen A, Fida H, Akhmedov S, Rasulbek E, Ataullaev Z. In Silico Study of Alkaloids as Potential Cyclin-Dependent Kinase (CDK) Inhibitors. 2025;1(4):324–35. Available from: https://jpscc.samipubco.com/article_235766_f9de3c3b67552b56d5e748fb40a24329.pdf
19. Khan S, Kale M, Siddiqui F, Nema N. Novel pyrimidine-benzimidazole hybrids with antibacterial and antifungal properties and potential inhibition of SARS-CoV-2 main protease and spike glycoprotein. Digit Chinese Med. 2021;4(2):102–19.
20. Shastri MA, Gadhave R, Talath S, Wali AF, Hani U, Puri S, et al. In silico Screening, Synthesis, and in vitro Enzyme Assay of Some 1,2,3-Oxadiazole-linke Tetrahydropyrimidine-5-carboxylate Derivatives as DPP-IV Inhibitors for Treatment of T2DM. Chem Methodol. 2024;8(11):800–19.
21. Suryawanshi RM, Shimpi RB, Muralidharan V, Nemade LS, Gurugubelli S, Baig S, et al. ADME, Toxicity, Molecular Docking, Molecular Dynamics, Glucokinase activation, DPP-IV, α-amylase, and α-glucosidase Inhibition Assays of Mangiferin and Friedelin for Antidiabetic Potential. Chem Biodivers [Internet]. 2025 Dec 23; Available from: https://onlinelibrary.wiley.com/doi/10.1002/cbdv.202402738
22. Suryawanshi RM, Shimpi RB, Muralidharan V, Nemade LS, Gurugubelli S, Baig S, et al. ADME, Toxicity, Molecular Docking, Molecular Dynamics, Glucokinase activation, DPP-IV, α-amylase, and α-glucosidase Inhibition Assays of Mangiferin and Friedelin for Antidiabetic Potential. Chem Biodivers. 2025;22(5).